



Observations of exoplanets and their atmospheres

G. Guilluy¹, M. Brogi^{1,2}, S. Desidera³, R. Gratton³, L. Pino⁴, and A. Ruggeri^{3,5}

¹ INAF – Osservatorio Astrofisico di Torino, Via Osservatorio 20, 10025, Pino Torinese, Italy

² Dipartimento di Fisica, Università degli Studi di Torino, via Pietro Giuria 1, I-10125, Torino, Italy

³ INAF – Osservatorio Astronomico di Padova, Vicolo dell'Osservatorio 5, 35122, Padova, Italy

⁴ INAF – Osservatorio Astrofisico di Arcetri, Largo E. Fermi 5, 50125, Firenze, Italy

⁵ Dipartimento di Fisica e Astronomia “Galileo Galilei”, Università di Padova, Vicolo dell'Osservatorio 3, IT-35122, Padova, Italy e-mail: gloria.guilluy@inaf.it

Received: 29 February 2024; Accepted: 18 June 2024

Abstract. The fields of exoplanetary science and astrochemistry are closely interconnected. Both the orbital architecture and the chemical atmospheric composition observed today are the result of intricate interactions among physical and dynamic processes occurring during planetary formation and subsequent migration. In this chapter, we deal with the scientific efforts conducted by the Italian community to extract exoplanetary properties, specifically orbital architecture and atmospheric composition, for both close-in and widely separated orbit exoplanets, based on their observed spectra. We will finally present the peculiar example of the binary system XO-2, where the atmospheric composition and the orbital architecture are strictly connected to the formation and migration history.

Key words. Planets and satellites: atmospheres - Planets and satellites: detections – techniques: spectroscopic - techniques: spectroscopic - techniques: radial velocities

1. Introduction

After nearly 30 years of exoplanet discoveries, exoplanetary science has transitioned from an early phase of planet-hunting (e.g., Fischer et al. 2014 and references therein) to a mature stage focused on determining planetary physical properties and understanding the origin of their remarkable diversity.

The observed orbital architecture arises from intricate interactions among diverse phys-

ical and dynamic processes occurring over various timescales during formation and subsequent orbital evolution. The planetary history does not solely alter orbital configurations; the composition of planetary atmospheres is also influenced by the chemical elements at the formation site and those encountered along the migration path, shaped by varying snowlines of oxygen and carbon-rich ices in the protoplanetary disk (e.g., Öberg et al. 2011; Madhusudhan et al. 2017).

An exoplanetary spectrum provides a window into the physical, chemical, and biological processes sculpting its past and influencing its future. Spectroscopic detection is crucial in unveiling the vast diversity of the exoplanet population and exploring potential extraterrestrial life beyond the Solar System (see e.g., Madhusudhan 2019 and references therein). Yet, obtaining exoplanetary spectra poses significant challenges. Exoplanets, being faint bodies, are frequently situated at sub-arcsecond orbital distances, obscured by the intense brightness of their host stars, which outshine them by several thousand to billions of times. Spectra of young and widely separated exoplanets (orbital separation $a > 10$ AU) discovered via *direct imaging* can be obtained directly by blocking or nulling the star's contribution using a coronagraph (Currie et al. 2023). Conversely, close-in orbit exoplanets cannot be spatially resolved from their host stars, given the significant difference in brightness. For these kinds of planets, measurements of time-varying signals are conducted. By monitoring changes in the combined star-plus-planet flux over time, the planetary spectrum can be extracted (e.g., Kreidberg 2018).

In this chapter, we delve into the scientific endeavours conducted in Italy to extract exoplanetary properties, specifically orbital architecture, and atmospheric composition, for both close-in and widely separated orbit exoplanets, based on their observed spectra. We start our discussion dealing with massive planets at wide separations (Sect. 2), to proceed with giant planets in close-in orbits (Sect. 3), which represent the focal points of atmospheric characterization investigations (Sect. 4). Finally, we conclude in Sect. 5 by presenting a unique binary system where the orbital arrangement resulting from formation and early evolution scenarios is intricately linked to its atmospheric composition.

2. Massive planets at large separations

2.1. Formation of Jupiter-like planets

How stellar, brown dwarf and planetary companions form and how this depends on the environment still need clarification. In Gratton et al. (2023) we combined high-contrast imaging and space astrometry finding that Jupiter-like (JL) planets are frequent in the β Pic moving group (BPMG) around stars where their orbit can be stable. In Gratton et al. (2024a) we expanded this analysis to other young nearby associations to determine the frequency, mass and separation of companions in general and JL in particular and their dependencies on the mass and age of the associations. Data about companions to stars in the BPMG and seven additional young associations were collected. The search completeness (the fraction of companions of a given mass ratio and separation actually discovered) was found to be very high for stellar companions but still required significant completeness corrections for JL companions. After these corrections (see Fig. 1), a high frequency of both stellar and JL companions was observed, clearly separated by a gap that corresponds to the well-known brown dwarf desert. Planetary companions pile up in the region just outside the ice line and we found them to be frequent (0.57 ± 0.11) once completeness was considered. The frequency of JL planets decreases with the overall mass and possibly the age of the association. We tentatively identify the populations of stellar and planetary companions as due to disk fragmentation and core accretion, respectively. The distributions of stellar companions with a semi-major axis < 1000 au is well explained by disk fragmentation. The observed trends with stellar mass can be attributed to a shorter, more intense phase of accretion onto the disk of massive stars and a steadier, prolonged accretion onto solar-type stars. Core accretion is identified as the likely mechanism for the formation of JL planets. To support this, in Gratton et al. (2024b) we considered updated dynamical masses and luminosities for sub-stellar objects in the BPMG. Cold-start evolutionary models, which assume low ini-

tial entropy (as it was expected for old core accretion models, Spiegel & Burrows 2012) do not reproduce the mass-luminosity relation for sub-stellar companions in the BPMG. This aligns rather closely with predictions from “hot start” scenarios which assume high initial entropy (that originally was thought to be a signature of disk instability scenarios, Spiegel & Burrows 2012). This is still consistent with the formation by core accretion. Figure 2 compares the observational data with the predictions of the theoretical core accretion models by Mordasini et al. (2017). These models show that even in this case a high initial entropy should be expected, due to the shocks that occurs at the interface between accreting gas and circumplanetary disks. The models by Mordasini et al. (2017) predict a range of initial entropies, depending on the exact history of every single planet; so rather than a single mass-luminosity relation, an intrinsic scatter of the luminosities is expected at each mass and age. In the figure, this is represented by the shaded area between the dashed lines. The comparison between models and observations is good, in view of the large uncertainties in individual points.

2.2. Spectrum of young directly imaged exoplanets

If planetary companions form through core accretion, their near-infrared (nIR) colour-magnitude diagrams might diverge from free-floating objects that rather formed as stars. The recent identification of a giant planet around AF Lep, part of the BPMG (Mesa et al. 2023), prompted us to re-examine this issue (Gratton et al. 2024b). We compared the properties of sub-stellar companions and free-floating objects in the BPMG and other young associations. We found a strong suggestion that the nIR colour-magnitude diagram for young companions is indeed different from that of free-floating objects belonging to the same young associations. This can be shown by remapping (i.e., transforming) coordinates from magnitudes and colours to effective temperature and the relevance of dust (r) (see Figure 3). This is achieved by interpolating the position of a sub-

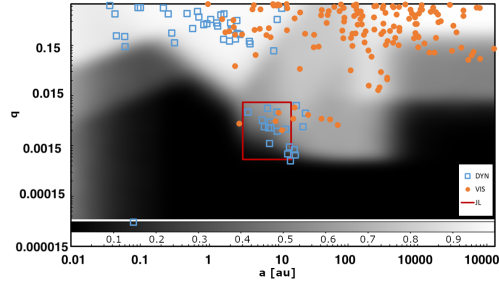


Fig. 1. Relation between semi-major axis a and mass ratio q between components for all companions found around stars that are members of the young associations considered in this paper. Filled orange circles are companions detected in imaging; open blue squares are those detected using dynamical methods or eclipses/transits. The companion detection completeness is in the background: the grey scale at the bottom of the figure indicates the level of completeness achieved in different regions of the $a - q$ plane. The red rectangle marks the area covered by JL planets. Figure from Gratton et al. (2024a)

stellar object in an nIR colour-magnitude diagram between the AMES-DUSTY (Chabrier et al. 2000) and AMES-COND (Allard et al. 2001) isochrones. These isochrones utilize the same internal AMES models (Baraffe et al. 1998), with a heavily dust-rich atmosphere for the AMES-DUSTY isochrone, and an atmosphere completely devoid of dust for the AMES-COND one. Therefore, a position near the AMES-COND isochrone ($r = 0$) indicates a dust-free atmosphere, whereas a position closer to the AMES-DUSTY atmosphere ($r = 1$) suggests a dust-rich atmosphere. Substellar objects start as hot objects with dust-rich atmospheres and L spectral types (their atmospheres are better represented by the AMES-DUSTY models, $r \gg 1$), and end as cool objects with dust-clean atmospheres and T spectral types (their atmospheres are better represented by the AMES-COND models, $r \sim 0$). The results in Figure 3 suggest that dust clearance from the atmosphere, which likely drives the transition between L and T spectral types, happens at a lower effective temperature (i.e.,

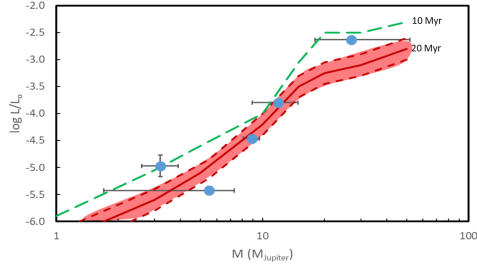


Fig. 2. Dynamical mass-luminosity relation for sub-stellar objects detected in the BPMG. The solid red and the dashed green lines are averages of the predictions by models of Mordasini et al. (2017) for ages of 20 and 10 Myr, respectively. The shaded red region between the dotted red lines represents the range of values that are expected for a 20 Myr age, depending on the peculiar evolution of individual objects. Figure from Gratton et al. (2024b)

later in their evolution) in young companions compared to free-floating objects. This difference might be tentatively attributed to variations in chemical composition.

3. Close-in transiting giant planets at young ages

Giant planets are expected to form at wide distances, mostly close to the snow line in the protoplanetary disks, and subsequently migrate towards their host stars. This could explain Hot Jupiters (HJ) and Warm Jupiters (WJ), gas planets with envelopes dominated in mass by H/He, and on very tight orbits, generally resulting in temperatures greater than 700 K. Two main classes of mechanisms have been proposed: migration within the protoplanetary disk (Lin et al. 1996) and migration through dynamical interactions with other planets or more massive, even stellar, objects (e.g., planet-planet scattering, Kozai interactions, dynamical interactions within the native cluster Weidenschilling & Marzari 1996; Wu et al. 2007).

The study of close-in giant planets at young ages allows us a better view of planetary migration processes. Several diagnostics can be

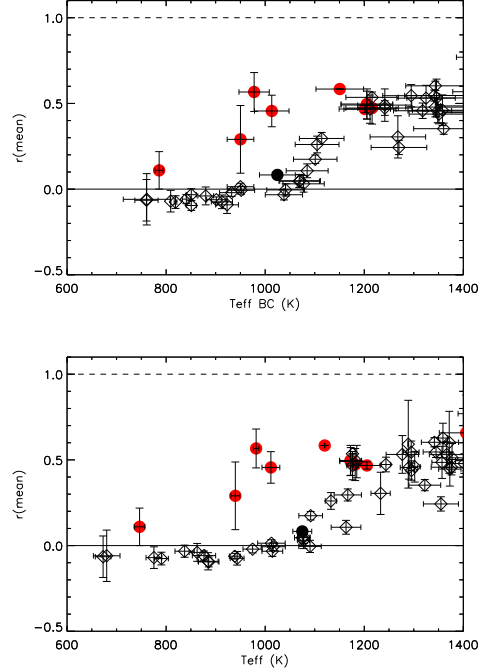


Fig. 3. Remapping of positions of stars from colour-magnitude diagram (cmd) into plan T_{eff} versus dust relevance parameter r for sub-stellar objects with ages in the range 10 – 200 Myr. The upper panel shows results obtained using T_{eff} obtained from luminosities derived from the K band magnitudes and bolometric corrections from Filippazzo et al. (2015), combined with evolutionary radii. The bottom panel shows T_{eff} from our remapping approach. In both panels, filled red circles are companions within 1000 au, filled black circles show companions outside 1000 au, and open diamonds show free-floating objects or very wide companions (separation > 1000 au). The solid and dashed lines represent the expectations for AMES-COND and AMES-DUSTY models. Figure from Gratton et al. (2024b)

evaluated, especially in the case of transiting planets: frequency of planets vs age, eccentricity and system obliquity (through the Rossiter-McLaughlin effect), without the alteration of tidal effects acting on Gyr timescales (Attia et al. 2023), and system architectures, extend-

ing to very wide orbit through direct imaging (e.g., Turrini et al. 2023; Desidera et al. 2023). In a few selected cases, the presence of debris disks provides additional constraints on system evolution (Engler et al. 2023).

High levels of magnetic activity in young host stars significantly limit blind searches and mass determination via radial velocity (RV) monitoring. However, this limitation can be mitigated for transiting planets with known orbital periods and phases through appropriate observing strategies and data modeling techniques (e.g., Foreman-Mackey et al. 2017; Nardiello et al. 2022). The stellar activity impact is instead much smaller for the transits detectability (Canocchi et al. 2023).

Furthermore, young late-type host stars emit high levels of high-energy radiation, which diminish over time due to magnetic braking. (Penz et al. 2008). This early emission can lead to significant evaporation of planetary atmospheres, altering the mass-radius relationship and creating a nearly empty region in the orbital period vs. planetary radius diagram. Indeed, there is preliminary evidence for the occurrence of low-density, evaporating planets, with some being relatively young (e.g., Benatti et al. 2021). However, a comprehensive understanding of the mass-loss mechanism has not yet been attained (e.g., Guilluy et al. 2024).

A dedicated program for the characterization of young transiting planets is being performed in the framework of the GAPS collaboration¹ exploiting the high-resolution (HR) spectra acquired with HARPS-N mounted on the Telescopio Nazionale Galileo (TNG) telescope (Carleo et al. 2020). Preliminary results from the project include the rebuttal of the claimed one order of magnitude higher frequency of HJs at few Myr with respect to old ages (Damasso et al. 2020), the mass determination of several young transiting planets, some of which are in multiple systems (e.g., Suárez Mascareño et al. 2021), the identification of planets undergoing significant mass loss

and for which a large shrinking of radius is expected (e.g., Mantovan et al. 2023) and of planets for which no further large-scale evaporation is expected (e.g., Damasso et al. *subm.*).

4. Characterization of exoplanetary atmospheres of close-in planets

Atmospheric characterisation of exoplanets, i.e. the determination of their chemical content and vertical thermal structure of the atmospheres, has been mostly focused on HJ. In first approximation, interpreting the spectra of this class of planets is much easier than for solar-system objects, in that, at their very high temperature, they are closer to thermochemical equilibrium, with a network of reactions that has been numerically computed since the late 1990s (Burrows & Sharp 1999) and subsequently simplified and expressed analytically (Madhusudhan 2012; Heng & Tsai 2016) also for different elemental ratios.

While equilibrium likely holds for planets within the 1,600-2,000 K temperature range, interpreting measured abundances becomes complicated outside this range due to other processes. At lower temperatures, silicates can form clouds after crossing the condensation curve, significantly affecting spectral features in transmission spectroscopy (Sing et al. 2016) and "shielding" radiation from lower atmospheric layers in emission, which influences the measured atmospheric temperature (Keating et al. 2019). At higher temperatures (1,800-2,200K), the condensation curves of TiO and VO are also crossed, which causes these species to be released in the gas phase. Since both are good optical absorbers, they can significantly contribute to heating up the upper atmosphere by shielding the incoming stellar radiation, causing thermal inversion layers (Fortney et al. 2008). At even higher temperatures (2,500K), molecules are thermally dissociated into atomic species and their additional opacity further contributes to thermal inversions. This category of planets is named ultra-hot Jupiters (UHJs), with the hotter members (≥ 2700 K) showing dominant sources of opacity commonly found in the stellar atmosphere such as H^- opacity (Arcangeli et al.

¹ In this chapter we focus on the research done within the framework of the GAPS collaboration as it has been presented during the CNAPII conferences

2018). These trends in the vertical thermal structure of exoplanets have now been measured on a large sample via low-resolution spectroscopy via the Wide Field Camera 3 of the Hubble Space Telescope (HST/WFC3) (Mansfield et al. 2021), and even directly via HR spectroscopy from the ground (e.g., Pino et al. 2020; Brogi et al. 2023). The study of UHJs will undoubtedly continue in the current decade both with ground- and space-based facilities. The former are particularly sensitive to individual atomic and molecular species due to the use of cross correlation as a selective filter (Birkby 2018), and UHJs offer the unprecedented opportunity to measure both volatiles (C, N, O) and refractory species (atoms heavier than He with the exclusion of volatiles). This allows linking the current atmospheric composition, with formation and early evolution scenarios. Predictions initially only relied on the C-to-O ratio as a tracer (Öberg et al. 2011; Mordasini et al. 2016), but were recently expanded to N chemistry and refractory materials to constrain both the distance at which planet formed and their subsequent enrichment by pebbles and/or planetesimals (Turrini et al. 2021). This is an open field currently, with the first measurements on single objects (Kasper et al. 2023; Ramkumar et al. 2023) and at the sample level (Gandhi et al. 2023) only recently presented. Space observations via the James Webb Space Telescope (JWST) are exquisitely placed to constrain the C-chemistry via the prominent CO₂ band at 4.2 μm , but the first results also show unexpected species detected, such as SO₂, opening up to sulphur chemistry (Rustamkulov et al. 2023). Besides the synergy in chemical measurements, space and ground observations can work in tandem to determine atmospheric dynamics. With the higher resolving power of ground spectroscopy, it is possible to resolve km/s winds directly (Snellen et al. 2010; Brogi et al. 2016; Pino et al. 2022). Measuring atmospheric dynamics is key to constraining the energy balance and the importance of drag processes, and therefore HR observations have been supported since the early detection by predictions from the modelling community (e.g., Showman et al. 2013). Part of the Italian GAPS program focuses

on characterizing exoplanetary atmospheres. The GAPS team is conducting transmission and emission spectroscopy on about thirty hot Jupiters and hot (sub-)Neptunes, covering a wide range of equilibrium temperatures (625–2500 K), hosted by stars of different spectral types (A to M with K magnitude ≤ 10.5 mag), to achieve the following objectives: (i) Identify atomic species to estimate the abundance of refractory elements (e.g. Pino et al. 2020) and/or to probe atmospheric expansion or escape, such as from the H α line (e.g., Borsa et al. 2021) and/or metastable helium triplet (e.g., Guilluy et al. 2024); (ii) Detect molecular compounds and estimate the atmospheric C/O ratio and metallicity, which provide constraints on planet formation and evolution scenarios (e.g. Giacobbe et al. 2021); (iii) Derive temperature-pressure profiles (e.g. Pino et al. 2020); and (iv) Detect the atmospheric Rossiter-McLaughlin effect (e.g. Borsa et al. 2019; Rainer et al. 2021).

5. A Case of Study: the binary system XO-2

A peculiar case that shows how the chemistry, and atmospheres in particular, are linked to the architecture of planetary systems is that of the binary system XO-2. Binary stars hosting planets are interesting per se because the two stars typically have the same characteristics and, therefore, we can do comparative studies. What's more, they might mutually affect the planetary systems of their companions. Unfortunately, only a very few cases of double planet-hosts are currently known and, among these, XO-2 is of remarkable interest. The system includes the two stars XO-2N and XO-2S, which have virtually the same mass and radius (almost identical to the Sun) and are both metal-rich ($Z > 2Z_{\odot}$), but the N component is significantly more metal-rich than the S one (e.g., Biazzo et al. 2015, Damasso et al. 2015). Regarding the architecture of the respective systems, XO-2N hosts a hot Jupiter ($m = 0.6 M_{\text{J}}$, $P = 2.6$ d, Burke et al. 2007), while XO-2S has a warm Saturn-like planet with $m \sin i = 0.26 M_{\text{J}}$ and $P = 18$ d, and a temperate Jupiter-like with $m \sin i = 1.38$

M_J and $P = 120$ d (Desidera et al. 2014). A very recent analysis (Ruggieri et al. 2024) based on an extended RV dataset found an additional Jupiter analog around XO-2S with $m \sin i \sim 3.7 M_J$ and $P \sim 13$ yr while confirming that there are no other detectable planets around XO-2N. These results imply that the planetary system of XO-2S is at least one order of magnitude more massive than that of XO-2N and this could be linked to the different metallicities of the two stars. Unfortunately, the authors did not detect any transits of the three planets orbiting XO-2S in the TESS light curves. As a result, it is impossible to determine their actual mass and radius, which in turn leads to an unconstrained chemical composition and poses difficulties in atmospheric studies. However, a solution can come from the atmosphere of the transiting hot Jupiter XO-2N b. Following Turrini et al. (2021), it is possible to reconstruct the giant planets' formation and migration histories using their elemental ratios involving C, O, and S, as done by, e.g., Biazzo et al. (2022). Several works have shown that these elemental ratios can be obtained with JWST observations (e.g., Bean et al. 2023 and Crossfield 2023). In the case of XO-2, JWST may aid in distinguishing between two scenarios. (i) XO-2S is deficient in heavy elements due to the rapid formation and migration of its two inner planets, which blocked the inward flux of dust but not of gas. The CNO elements should not be affected at this point but, later on, the third planet blocks them outside of the snow line. In this scenario, it is unlikely that XO-2N has been enriched in metals compared to the proto-stellar cloud from which it formed, and XO-2N b is expected to have sub-stellar metallicity; (ii) In the other case, we have a metal enrichment for XO-2N because its planet formed and migrated relatively late without affecting the inward dust flux. In this scenario, XO-2N b should be CNO-rich (super-stellar) while sulfur should be almost absent. The binary system XO-2 is thus a remarkable example of how chemistry, and the study of atmospheres, in particular, can greatly contribute to the understanding of how planetary systems form and evolve.

Acknowledgements. This work has been supported by the PRIN-INAF 2019.

References

- Allard, F., Hauschildt, P. H., Alexander, D. R., Tamanai, A., & Schweitzer, A. 2001, *ApJ*, 556, 357
- Arcangeli, J., Désert, J.-M., Line, M. R., et al. 2018, *ApJ*, 855, L30
- Attia, O., Bourrier, V., Delisle, J. B., & Eggenberger, P. 2023, *A&A*, 674, A120
- Baraffe, I., Chabrier, G., Allard, F., & Hauschildt, P. H. 1998, *A&A*, 337, 403
- Bean, J. L., Xue, Q., August, P. C., et al. 2023, *Nature*, 618, 43
- Benatti, S., Damasso, M., Borsa, F., et al. 2021, *A&A*, 650, A66
- Biazzo, K., D'Orazi, V., Desidera, S., et al. 2022, *Astronomy & Astrophysics*, 664, A161
- Biazzo, K., Gratton, R., Desidera, S., et al. 2015, *A&A*, 583, A135
- Birkby, J. L. 2018, in *Handbook of Exoplanets*, ed. H. J. Deeg & J. A. Belmonte, 16
- Borsa, F., Rainer, M., Bonomo, A. S., et al. 2019, *A&A*, 631, A34
- Brogi, M., de Kok, R. J., Albrecht, S., et al. 2016, *ApJ*, 817, 106
- Brogi, M., Emeka-Okafor, V., Line, M. R., et al. 2023, *AJ*, 165, 91
- Burke, C. J., McCullough, P. R., Valenti, J. A., et al. 2007, *ApJ*, 671, 2115
- Burrows, A. & Sharp, C. M. 1999, *ApJ*, 512, 843
- Canocchi, G., Malavolta, L., Pagano, I., et al. 2023, *A&A*, 672, A144
- Carleo, I., Malavolta, L., Lanza, A. F., et al. 2020, *A&A*, 638, A5
- Chabrier, G., Baraffe, I., Allard, F., & Hauschildt, P. 2000, *ApJ*, 542, 464
- Crossfield, I. J. M. 2023, *The Astrophysical Journal Letters*, 952, L18
- Currie, T., Biller, B., Lagrange, A., et al. 2023, in *Astronomical Society of the Pacific Conference Series*, Vol. 534, *Protostars and Planets VII*, ed. S. Inutsuka, Y. Aikawa, T. Muto, K. Tomida, & M. Tamura, 799
- Damasso, M., Biazzo, K., Bonomo, A. S., et al. 2015, *A&A*, 575, A111

- Damasso, M., Lanza, A. F., Benatti, S., et al. 2020, *A&A*, 642, A133
- Damasso, M., Locci, D., Benatti, S., & et al. subm.
- Desidera, S., Bonomo, A. S., Claudi, R. U., et al. 2014, *A&A*, 567, L6
- Desidera, S., Damasso, M., Gratton, R., et al. 2023, *A&A*, 675, A158
- Engler, N., Milli, J., Gratton, R., et al. 2023, *A&A*, 672, A1
- Filippazzo, J. C., Rice, E. L., Faherty, J., et al. 2015, *ApJ*, 810, 158
- Fischer, D. A., Howard, A. W., Laughlin, G. P., et al. 2014, in *Protostars and Planets VI*, ed. H. Beuther, R. S. Klessen, C. P. Dullemond, & T. Henning, 715–737
- Foreman-Mackey, D., Agol, E., Ambikasaran, S., & Angus, R. 2017, *AJ*, 154, 220
- Fortney, J. J., Lodders, K., Marley, M. S., & Freedman, R. S. 2008, *ApJ*, 678, 1419
- Gandhi, S., Kesseli, A., Zhang, Y., et al. 2023, *AJ*, 165, 242
- Giacobbe, P., Brogi, M., Gandhi, S., et al. 2021, *Nature*, 592, 205
- Gratton, R., Bonavita, M., Mesa, D., et al. 2024a, *A&A*, 685, A119
- Gratton, R., Bonavita, M., Mesa, D., et al. 2024b, *A&A*, 684, A69
- Gratton, R., Mesa, D., Bonavita, M., et al. 2023, *Nature Communications*, 14, 6232
- Guilluy, G., D’Arpa, M. C., Bonomo, A. S., et al. 2024, *A&A*, 686, A83
- Heng, K. & Tsai, S.-M. 2016, *ApJ*, 829, 104
- Kasper, D., Bean, J. L., Line, M. R., et al. 2023, *AJ*, 165, 7
- Keating, D., Cowan, N. B., & Dang, L. 2019, *Nature Astronomy*, 3, 1092
- Kreidberg, L. 2018, in *Handbook of Exoplanets*, ed. H. J. Deeg & J. A. Belmonte, 100
- Lin, D. N. C., Bodenheimer, P., & Richardson, D. C. 1996, *Nature*, 380, 606
- Madhusudhan, N. 2012, *ApJ*, 758, 36
- Madhusudhan, N. 2019, *ARA&A*, 57, 617
- Madhusudhan, N., Bitsch, B., Johansen, A., & Eriksson, L. 2017, *MNRAS*, 469, 4102
- Mansfield, M., Line, M. R., Bean, J. L., et al. 2021, *Nature Astronomy*, 5, 1224
- Mantovan, G., Malavolta, L., Desidera, S., et al. 2023, arXiv e-prints, arXiv:2310.16888
- Mesa, D., Gratton, R., Kervella, P., et al. 2023, *A&A*, 672, A93
- Mordasini, C., Marleau, G. D., & Mollière, P. 2017, *A&A*, 608, A72
- Mordasini, C., van Boekel, R., Mollière, P., Henning, T., & Benneke, B. 2016, *ApJ*, 832, 41
- Nardiello, D., Malavolta, L., Desidera, S., et al. 2022, *A&A*, 664, A163
- Öberg, K. I., Murray-Clay, R., & Bergin, E. A. 2011, *ApJ*, 743, L16
- Penz, T., Micela, G., & Lammer, H. 2008, *A&A*, 477, 309
- Pino, L., Brogi, M., Désert, J. M., et al. 2022, *A&A*, 668, A176
- Pino, L., Désert, J.-M., Brogi, M., et al. 2020, *ApJ*, 894, L27
- Rainer, M., Borsa, F., Pino, L., et al. 2021, *A&A*, 649, A29
- Ramkumar, S., Gibson, N. P., Nugroho, S. K., Maguire, C., & Fortune, M. 2023, *MNRAS*, 525, 2985
- Ruggieri, A., Desidera, S., Biazzo, K., et al. 2024, *A&A*, 684, A116
- Rustamkulov, Z., Sing, D. K., Mukherjee, S., et al. 2023, *Nature*, 614, 659
- Showman, A. P., Fortney, J. J., Lewis, N. K., & Shabram, M. 2013, *ApJ*, 762, 24
- Sing, D. K., Fortney, J. J., Nikolov, N., et al. 2016, *Nature*, 529, 59
- Snellen, I. A. G., de Kok, R. J., de Mooij, E. J. W., & Albrecht, S. 2010, *Nature*, 465, 1049
- Spiegel, D. S. & Burrows, A. 2012, *ApJ*, 745, 174
- Suárez Mascareño, A., Damasso, M., Lodieu, N., et al. 2021, *Nature Astronomy*, 6, 232
- Turrini, D., Marzari, F., Polychroni, D., et al. 2023, *A&A*, 679, A55
- Turrini, D., Schisano, E., Fonte, S., et al. 2021, *The Astrophysical Journal*, 909, 40
- Weidenschilling, S. J. & Marzari, F. 1996, *Nature*, 384, 619
- Wu, Y., Murray, N. W., & Ramsahai, J. M. 2007, *ApJ*, 670, 820